ELSEVIER

Journal of Fluids and Structures 23 (2007) 39–57

JOURNAL OF FLUIDS AND STRUCTURES

www.elsevier.com/locate/jfs

Cross-flow past a pair of nearly in-line cylinders with the upstream cylinder subjected to a transverse harmonic oscillation

S.J. Price*, M.P. Païdoussis, S. Krishnamoorthy

Department of Mechanical Engineering, McGill University, Montréal, Québec, Canada H3A 2K6

Received 2 September 2005; accepted 8 July 2006
Available online 24 October 2006

Abstract

An experimental investigation is presented for the cross-flow past a pair of staggered circular cylinders, with the upstream cylinder subject to forced harmonic oscillation transverse to the flow direction. Experiments were conducted in a water tunnel with Reynolds numbers, based on upstream velocity, U, and cylinder diameter, D, in the range $1440 \leqslant \mathrm{Re} \leqslant 1680$. The longitudinal separation between cylinder centres is $L/D = 2.0$, with a transverse separation (for the mean position of the upstream cylinder) of $T/D = 0.17$; the magnitude of the harmonic oscillation is $0.44D$ peak-to-peak and the nondimensional frequency range of the excitation is $0.05 \leqslant f_e D/U \leqslant 0.44$. Flow visualization of the wake-formation region and hot-film measurements of the wake spectra are used to investigate the wake-formation process. An earlier study showed that stationary cylinders in this nearly in-line configuration straddle two very different flow regimes, the so-called *shear-layer reattachment* (SLR) and *induced separation* (IS) regimes. The present study, demonstrates that oscillation of the upstream cylinder causes considerable modification of the flow patterns around the cylinders. In particular, the wake experiences strong periodicities at the frequency of the oscillating cylinder; in addition to the usual fundamental lock-in, both sub- and superharmonic resonances are obtained. It is also observed that, although the flow exhibits regions of SLR and IS for excitation frequencies below the fundamental lock-in, for frequencies above the lock-in range the flow no longer resembles either of these flow regimes and vortices are formed in the gap between the cylinders.

Keywords: Staggered cylinder pair; Flow visualization; Flow patterns; Oscillating upstream cylinder; Shear-layer reattachment; Induced separation; Fundamental resonance; Subharmonic resonance; Superharmonic resonance; Lock-in

1. Introduction

Although less well studied than the flow around an isolated circular cylinder, the flow around small groups of cylinders in close proximity to each other has received considerable attention in recent years. These studies have identified a number of key differences in this more complex flow compared to that for isolated cylinders. In particular,

*Corresponding author.
E-mail address: Stuart.Price@mcgill.ca (S.J. Price).

0889-9746/$ - see front matter © 2006 Elsevier Ltd. All rights reserved.
doi:10.1016/j.jfluidstructs.2006.07.006

as discussed in review articles by Nishimura (1986), Zdravkovich (1987, 1993) and Ohya et al. (1989), the flow around interacting cylinders may involve complex interactions between the shear-layers, vortices and Kármán vortex streets.

A first attempt at classifying this type of flow for two staggered cylinders was made by Zdravkovich (1987), who, depending on the relative separation of the cylinders, identified three different flow regimes: (i) *no interference*; (ii) *wake interference*, where one of the cylinders is partially or completely submerged in the wake of the other; and (iii) *proximity interference*, where the two cylinders are located close to each other but neither is in the wake of the other. Gu and Sun (1999) extended this classification and subdivided the wake interference region into two: *shear-layer interference* and *neighbourhood interference*.

Using a combination of flow visualization and particle image velocimetry, Sumner et al. (2000) suggested that the flow around two closely spaced cylinders is much more complex than suggested by either Zdravkovich or Gu and Sun. They found that, depending on cylinder orientation, there are *nine* different flow patterns. These involve different processes of shear-layer reattachment (SLR), induced separation (IS), vortex pairing and synchronization, and vortex impingement. This study also suggested that the so-called vortex-shedding frequencies in the near-wake are more properly associated with flow periodicities of individual shear-layers than with bulk wake periodicities of individual cylinders; specifically, the two shear-layers shed from the downstream cylinder often have periodicities occurring at different frequencies.

The nine different flow patterns identified by Sumner et al. (2000) can be grouped into three broad categories: (a) *single bluff-body flows*; (b) *flow patterns at small angles of incidence* ($\alpha = 0$–30° depending on P/D); and (c) *flow patterns for large angles of incidence* ($\alpha = 20$–90° depending on P/D). (The relative separation between two cylinders is typically characterized by either the flow incidence angle, α, and pitch, P, or the longitudinal, L, and transverse, T, separation; see Fig. 1.) For "single bluff-body" flows, the two cylinders are close enough to behave as one body, although there may be some base-bleed between them. The "small incidence" flows, except at large values of P/D, are characterized by suppression of both the vortex shedding from the upstream cylinder and the gap-flow between cylinders; for Reynolds numbers in the high sub-critical range, these small incidence flows are known to produce large changes of the lift and drag coefficients on the downstream cylinder with relatively small changes in T/D (Ting et al., 1998). At "large angles of incidence", vortex shedding occurs from each of the cylinders, a gap-flow exists, and there may be two dominant flow periodicities in the wake.

Some related experimental work by Bouak and Lemay (1998) showed that a small cylinder placed upstream of a larger cylinder (the ratio of cylinder diameters was 1/8), with incidence angle of less than 20°, can have a significant effect on the static force coefficients of the larger downstream cylinder, as well as the flow structure around it.

Bearing in mind the additional complexity of the flow around a single cylinder forced to oscillate transverse to the flow, for example see Krishnamoorthy et al. (2001), it is expected that the flow around a pair of cylinders will also be more complex when either one or both of the cylinders are forced to oscillate or allowed to vibrate in response to the flow. For a single cylinder undergoing such an oscillation the focus of research has often been on the "lock-in" phenomenon, where for excitation frequencies, f_e, close to the stationary cylinder's vortex-shedding frequency, f_{os}, the vortex shedding is synchronized with the oscillation frequency of the cylinder. These studies have included elastically mounted cylinders in cross-flow (Feng, 1968; Brika and Laneville, 1993; Khalak and Williamson, 1997), forced harmonic oscillation of the cylinders (Koopmann, 1967; Stansby, 1976; Bearman and Currie, 1979; Ongoren and Rockwell, 1988; Williamson and Roshko, 1988; Gu et al., 1994; Carberry et al., 2001) and numerical simulations of the flow (Lu and Dalton, 1996; Blackburn and Henderson, 1999).

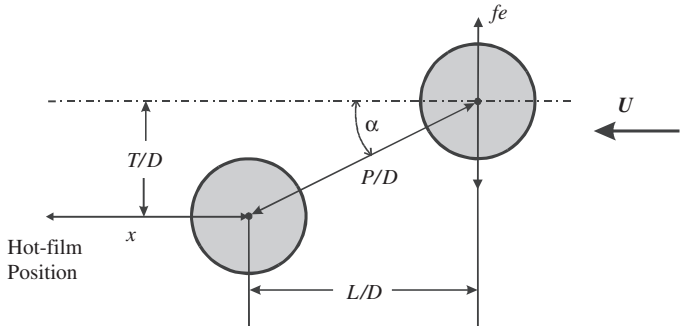

Fig. 1. Schematic of the pair of cylinders, and location of the hot-film probe.

Associated with this lock-in region is a peak in the vortex-induced forces on the cylinder. In addition, a small change in f_e produces approximately a 180° change in phase between the vortex induced force and the cylinder displacement [see, for example, Koopmann (1967) and Ongoren and Rockwell (1988)].

Using flow visualization, Williamson and Roshko (1988) observed a number of different modes of vortex shedding for a cylinder subject to transverse forcing. These depended on both the amplitude of oscillation and the frequency ratio f_e/f_{os}, and were characterized according to the number of vortex pairs, "P", or single vortices, "S", shed into the wake per cycle of cylinder motion. Williamson and Roshko associated the sudden change in phase with increasing f_e to a switch from the "2P" mode (where four vortices are shed per cycle of cylinder oscillation, giving rise to a vortex street of two vortex pairs) to a "2S" mode (where two single vortices are shed per cycle of cylinder oscillation, giving rise to a Kármán-type vortex street). The origin of these two different modes is connected with the timing of vortex formation relative to cylinder oscillation. Every half-cycle of cylinder motion, vortex roll-ups occur from each shear-layer; thus, four vortices are shed every cycle of oscillation. The 2S pattern results when the timing of the vortex roll-up is such that two like-sign vortices coalesce to form *two vortices per cycle* of cylinder oscillation. When the timing of the vortex-formation process is such that vortices of opposite sign vorticity pair up to give *two vortex pairs per cycle*, the 2P pattern results. It should be noted, however, that Ongoren and Rockwell (1988) report Kármán vortex streets, or 2S modes, on either side of the phase switch. In addition, the numerical simulations of Blackburn and Henderson (1999) did not predict the 2P mode, although this may have been a consequence of assuming a two-dimensional (2-D) flow. In a CFD study of a flexibly mounted 2-D cylinder at $\mathrm{Re} = 200$, conducted using a discrete vortex method, Zhou et al. (1999) obtained both 2S and S + P wakes depending on f_e/f_{os}.

Both Gu et al. (1994) and Carberry et al. (2001) observed that the increase in vortex-induced force with increasing f_e/f_{os} was accompanied by a significant change in the near-wake topology. As f_e/f_{os} increased in the range $f_e/f_{os} \approx 1$, the wake vorticity moved closer to the cylinder, and reached a limiting condition, which resulted in an abrupt switch of vorticity to the other side of the cylinder; this was also observed in the numerical simulations of Lu and Dalton (1996). Carberry et al. (2001) also clearly show that this switch of vorticity is accompanied by a switch from a 2P to a 2S mode.

In addition to primary lock-in, a number of authors experimenting with cylinders subject to forced oscillations have observed sub- and superharmonic lock-ins. For example, Stansby (1976) observed a "secondary" lock-in, where the vortex-shedding frequency was half the excitation frequency, $f_o = \frac{1}{2} f_e$, corresponding to a 2-superharmonic forcing, and a "tertiary" lock-in, where $f_o = \frac{1}{3} f_e$, corresponding to a 3-superharmonic forcing; while tertiary lock-in occurred over a wide range of forcing frequencies, the secondary lock-in did not.

Williamson and Roshko (1988) observed that, as the freestream velocity was increased beyond the 2S and 2P regimes, no synchronized vortex pattern was observed until the oscillation frequency corresponded to a $\frac{1}{3}$-subharmonic forcing, $f_o = 3f_e$, where a 2P + 2S synchronized vortex pattern comprising six vortices (two vortex pairs and two single vortices) was observed. The reason why a synchronized vortex pattern of four vortices, corresponding to $\frac{1}{2}$-subharmonic forcing, is not possible is explained by using symmetry arguments.

Ongoren and Rockwell (1988) observed synchronization (phase-locking) of the *near-wake structure* to the cylinder motion both for $\frac{1}{2}$-subharmonic forcing ($f_o = 2f_e$), when vortex shedding from the shear-layers repeats every half-cycle of cylinder displacement, and for harmonic forcing, $f_o = f_e$, when vortex shedding repeats every full cycle. The perturbed near-wake was observed to recover rapidly to an antisymmetric Kármán vortex street over a wide range of oscillation frequencies, varying from subharmonic to 4-superharmonic, $f_o = \frac{1}{4} f_e$, forcing.

Krishnamoorthy et al. (2001) considered oscillation frequencies f_e ranging from $\frac{1}{3}$-subharmonic to 3-superharmonic excitation. It was shown that, as f_e was incremented within the fundamental lock-in regime, the structure of the formation region underwent two distinct transitions. The first, accompanied by an abrupt reduction in vortex formation length, corresponded to a switch from a 2P wake to a 2S wake. After a subsequent transition at a slightly higher f_e, the phase of vortex shedding relative to the cylinder displacement switched by about 180°. Between the two transitions, the vortex formation length was a minimum. A similar minimum in vortex formation length was also attained when f_e was increased to a 3-superharmonic synchronization. In addition, although both the $\frac{1}{3}$- and $\frac{1}{2}$-subharmonic excitation produced formation regions which are periodic with every cycle of cylinder oscillation, a synchronized wake pattern forms only in the former case.

There have also been a few experimental studies which have examined the wake characteristics behind a pair of cylinders when one or both of them are subject to forced oscillation. Mahir and Rockwell (1996a, b) examined the near-wake structure of tandem (1996a) and side-by-side (1996b) cylinder pairs for $\mathrm{Re} = 160$, with both cylinders subjected to transverse oscillations. The effect of frequency and amplitude of oscillation, phase between the cylinders, and separation between the cylinders were examined via a combination of hydrogen-bubble flow visualization and wake spectral measurements. For the tandem arrangement, lock-in was obtained for $P/D = 2.5$ and 5 over the complete range of phase angle between the cylinders (0–180°). For the larger spacing between cylinders ($P/D = 5$), the range of lock-in in the amplitude–frequency plane was approximately the same as for a single cylinder; however, for the small spacing,

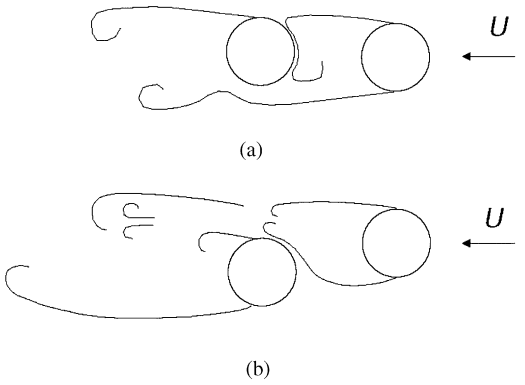

Fig. 2. Schematic showing (a) the *shear-layer reattachment* (SLR) and (b) *induced separation* (IS) flow regimes.

lock-in occurred over a wider range of frequencies. The side-by-side configuration also exhibited lock-in for sufficiently large cylinder separation ($P/D = 3$), but was not observed for smaller values. Within the lock-in range the wake spectra for both configurations showed a dominance of frequency peaks at the forcing frequency and its harmonics, but outside of the lock-in range there was significant modulation of the frequency peaks (with the modulation frequency being the difference between the cylinder oscillation frequency and the vortex-shedding frequency).

Lai et al. (2003) also investigated the wake structure of two side-by-side cylinders, but with only one of them subject to transverse oscillations. Their experiments, for Reynolds numbers in the range 150–1000, included wake spectral measurements, particle image velocimetry measurements and flow visualization. For $P/D = 3.5$ they observed that the lock-in range of the wake behind the oscillating cylinder was similar to that for a single cylinder; lock-in also occurred for the wake behind the stationary cylinder but for a narrower frequency range. For $P/D = 2.2$ there was considerably more interaction between the two wakes and lock-in occurred over an expanded frequency range compared with that for a single cylinder.

Recently, Sumner and Richards (2003) presented an investigation of the steady lift and drag coefficients and Strouhal numbers for a pair of staggered cylinders with $P/D = 2.0$ and 2.5 and α ranging from 0° to 90°; the Reynolds number in their experiments was either 3.2×10^4 or 7.0×10^4. A more extensive investigation was presented by Sumner et al. (2005) covering a wider range of Reynolds number and P/D.

Alam and Sakamoto (2005) and Alam et al. (2005) used standard Fourier methods and wavelets to analyse the surface pressure measurements on cylinders in a staggered arrangement. Their experiments were conducted for a wide range of α and P/D at $\mathrm{Re} = 5.5 \times 10^4$.

The aim of the present study is to investigate the near-wake structure and synchronization phenomena for a pair of staggered circular cylinders when the upstream cylinder is subjected to transverse excitation. The configuration chosen has a longitudinal separation between cylinder centres of $L/D = 2.0$, and nominal transverse separation (for the mean position of the upstream cylinder) of $T_{\mathrm{nom}}/D = 0.17$ ($\alpha_{\mathrm{nom}} = 5.0^\circ$, $P_{\mathrm{nom}}/D = 2.0$, see Fig. 1). The results of Sumner et al. (2000) indicate that for $L/D = 2.0$ and for this range of T/D the flow is always a *small incidence* type flow, and that the flow belongs to (i) the SLR regime for $T/D < 0.35$, and (ii) to the IS regime for $T/D > 0.35$. As sketched in Fig. 2, in the SLR regime the shear-layer shed from the inner side of the upstream cylinder reattaches on the downstream cylinder, and there is no gap-flow between the cylinders. As the incidence between the cylinders is increased, the SLR can no longer be maintained; instead, the inner shear-layer is deflected through the gap between the cylinders, resulting in the IS flow pattern. For both of these flow configurations there is a vortex street shed downstream of the cylinder pair, and the flow is characterized by a single Strouhal number of approximately 0.17 (Sumner et al., 2000). The primary objective of the present study is to determine the effect of an oscillating upstream cylinder on these flow regimes, and to investigate the existence of resonances, both sub- and superharmonic as well as fundamental, between the wake structure and the cylinder oscillation; hence, the range of frequency of oscillation was $0.05 \leqslant f_e D/U \leqslant 0.44$.

2. Experimental procedure

As discussed in the Introduction, experiments were conducted for a pair of circular cylinders in cross-flow, with the downstream cylinder fixed in place and the upstream one subject to forced harmonic oscillation transverse to the

flow direction; see Fig. 1. The longitudinal and transverse separation between cylinder centres was $L/D = 2.0$ and $T_{nom}/D = 0.17$.

The experiments were carried out in a closed-circuit Kempf and Remmers water tunnel, with a test-section 1100 mm long and 254×254 mm in cross-section. Flow in the test-section has a streamwise turbulence intensity of 0.5% and a velocity profile uniformity of better than 95%. The freestream velocity U was measured using a miniature "turbine" flow meter, designed to measure very low flow velocities (40–150 mm/s).

The two cylinders were supported vertically in the test-section. The downstream cylinder was fixed, and the upstream one was mounted on a scotch-yoke mechanism, enabling forced harmonic oscillation transverse to the flow direction. A complete description of the scotch-yoke mechanism, cylinder mounting, etc. is given by Krishnamoorthy et al. (2001); suffice it to say that the possible oscillation frequency, f_e, range, was 0.2–4.9 Hz with half peak-to-peak amplitude of 7.0 mm ($0.22D$). Considerable care was taken in the design and construction of the scotch-yoke mechanism, to ensure that the cylinder motion was essentially a pure sine wave over this range of frequencies.

Both cylinders were constructed from plexiglas rod of 16 mm diameter; the cylinder aspect ratio was 16. The solid blockage ratio per cylinder was 6.3%, and so the maximum possible blockage was 12.6%; however, for the present configuration the effective blockage was always less than this maximum value. No end plates were fitted to the cylinders.

Flow visualization was carried out using the same techniques as in Sumner et al. (2000). Rhodamine dye, which is fluorescent, was injected into the boundary layer at mid-span of either the upstream or downstream cylinder; however, the most revealing results tended to be obtained when the dye was injected from the upstream cylinder. The dye was injected through a pair of ports 120° apart, oriented facing upstream and symmetrically located with respect to the free-stream. The dye flow-rate was controlled by a needle valve in the gravity-feed line feeding the ports. The plane of the test-section where the dye was released was illuminated by a xenon arc lamp, giving a 12–15 mm thick light sheet. A professional S-VHS video camera was used to record the wake structure revealed by the dye; this enabled detailed interpretation of the flow-field to be conducted later, and also allowed individual instantaneous images to be obtained, as presented in this paper. Using a video camera, as opposed to a still camera, which would have produced higher quality images, enabled time series of the flow to be recorded; these video recordings proved to be invaluable when attempting to characterize the dynamics of the flow.

In addition to the flow-visualization, spectral measurements were made in the wake of the cylinders using a hot-film anemometer. The output from the hot-film was analyzed to obtain velocity power spectra with a frequency resolution of 12.5 mHz. Preliminary experiments were conducted with the cylinders stationary for locating an appropriate position for the hot-film to give a strong signal at the vortex-shedding frequency. The position was selected to be on the centre-line of the downstream cylinder and $x/D = 4.7$ downstream of its centre; see Fig. 1. All wake spectra presented in this paper, for both the stationary and oscillating cylinders, were measured at this location.

Initially, a set of experiments was conducted with the cylinders stationary; these were done with the cylinders aligned at a range of T between T_{max} and T_{min}. Then, f_e was incrementally varied such that the frequencies of the various synchronization regimes were spanned.

For all of the experimental results presented here, the flow velocity was kept approximately constant in the range 91–107 mm/s, giving a Reynolds number range of $1440 \leqslant Re \leqslant 1680$. This corresponds to the low sub-critical Reynolds number range for a solitary cylinder. This range of Re was selected based on two practical limitations. Firstly, at higher velocities the dye tended to diffuse more rapidly, leading to a reduction in quality of the visualization images. Secondly, as previously mentioned, the oscillation frequency range for the scotch-yoke mechanism is 0.2–4.9 Hz; hence, to achieve the desired range of f_eD/U also imposes a maximum value of Re.

3. Results and discussion

As the upstream cylinder oscillates the value of T/D varies. For the amplitude of oscillation considered, the maximum is $T_{max}/D = 0.39$ and the minimum $T_{min}/D = -0.05$. As discussed in the Introduction, the results of Sumner et al. (2000) indicate that for $L/D = 2.0$ and for this range of T/D the flow is always a *small incidence* type flow, and that the flow belongs to (i) the SLR regime for $T/D < 0.35$, and (ii) to the IS regime for $T/D > 0.35$.

3.1. Stationary cylinders

Sample flow visualization images with the cylinders fixed at both the maximum and minimum values of T/D are shown in Fig. 3, and wake spectra are presented in Fig. 4 for four different values of T/D.

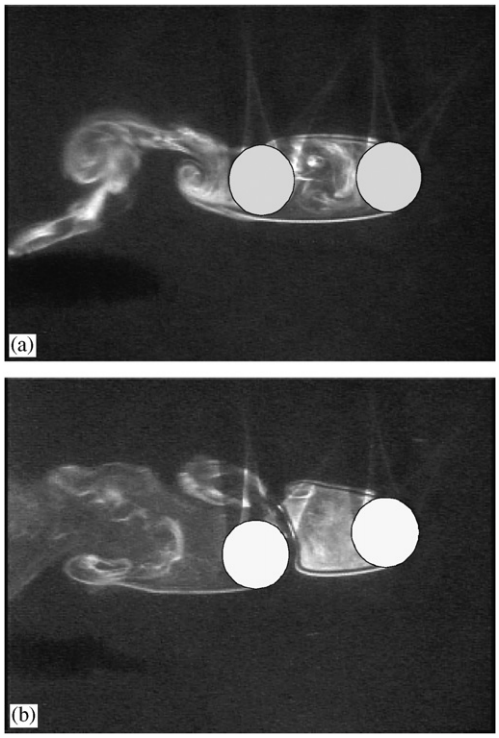

Fig. 3. Flow visualization images with the upstream cylinder stationary: (a) $T/D = -0.05$ (T_{min}), *shear-layer reattachment* (SLR) regime; (b) $T/D = 0.39$ (T_{max}), *induced separation* (IS) regime.

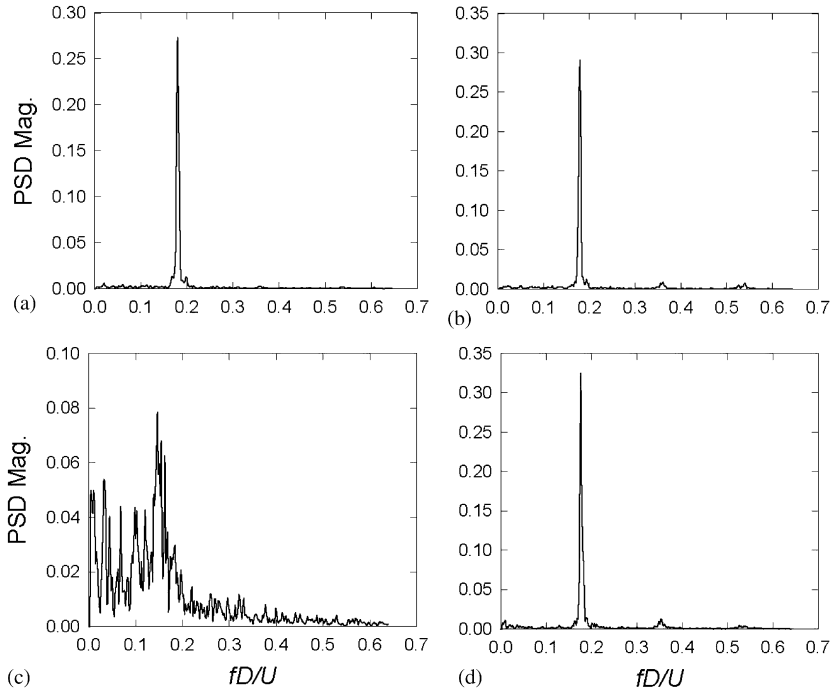

Fig. 4. Spectra measured in the wake of the static cylinders for various values of T/D: (a) $T/D = -0.05$ (T_{min}); (b) $T/D = 0.0$; (c) $T/D = 0.39$ (T_{max}); (d) $T/D = 0.17$ (T_{nom}).

As observed in Fig. 3(a) for the flow visualization at T_{min}/D (−0.05), the shear-layer shed from the inside (lower) surface of the upstream cylinder reattaches onto the outside (lower in the figure) surface of the downstream cylinder, and there is no gap-flow between the cylinders. This indicates that this flow belongs to the SLR regime (see Fig. 2(a)). Observations from the video recording indicate that the shear-layer shedding from the downstream cylinder occurs at the same frequency as the dominant periodicity for the far-wake vortex street. Also, the shear-layers shed from the upstream cylinder reattach onto the downstream cylinder in a manner that is synchronized with the far-wake vortex pattern. In the wake spectrum for this configuration (Fig. 4(a)) there is one dominant peak, indicating a Strouhal number of $St = 0.178$.

The flow visualization with the cylinders statically held at T_{max}/D (0.39), presented in Fig. 3(b), indicates that there are two significant differences for this flow compared with that for T_{min}/D. Most noticeable is that the lower shear-layer shed from the upstream cylinder is deflected in front of the downstream one. In addition, flow separation occurs from the inside surface of the downstream cylinder. These features are characteristic of the IS flow regime (Fig. 2(b)). A comparison of Figs. 3(a) and (b) shows that for T_{max}/D, in contrast to the case for T_{min}/D, the downstream wake is disorganized and does not exhibit a well-defined vortex formation process. This is also illustrated by the broad-band power spectrum of the wake signal of Fig. 4(c); nevertheless, it is still possible to obtain a Strouhal number for this case, $St = 0.145$.

Additional wake spectral measurements were conducted at intermediate values of T/D, and are presented in Figs. 4(b) and (d). In both cases there is one dominant peak, giving $St = 0.178$ and 0.175 at $T/D = 0.0$ and 0.17, respectively. These values are similar to the Strouhal number obtained at $T/D = -0.05$, suggesting that for $L/D = 2.0$ the T/D—boundary between the SLR and IS regimes is somewhere between 0.17 and 0.39. Sumner et al. (2000) suggested that the SLR region extends to approximately $T/D = 0.35$, which is consistent with the present results.

As discussed in the preceding, the frequency spectra measured in the wake of the stationary cylinders indicates that for $-0.05 \leqslant T/D \leqslant 0.17$ the Strouhal number is reasonably constant, varying from 0.178 to 0.175, and at $T/D = 0.39$ the Strouhal number is 0.145. These results are consistent with the results of Sumner et al. (2000) who obtained $St = 0.177$ at $T/D = 0.00$ for $1260 \leqslant Re \leqslant 1350$. At higher Reynolds numbers, $Re = 3.2 \times 10^4$, 5.4×10^4 and 7.2×10^4, Sumner and co-workers (Sumner and Richards, 2003; Sumner et al., 2005; Sumner, 2006) obtained St varying from 0.14 to 0.27 (with the majority of the results falling in the range 0.16–0.17) as α was varied from 0° to 12° with $P/D = 2.0$ (corresponding to T/D varying from 0 to 0.42). Sumner's results also indicate that, as α is increased past approximately 6° ($T/D = 0.21$), the wake spectral PSDs become very broad-banded, making it difficult to determine the Strouhal number; this is consistent with the results shown in Fig. 4(c). Hence, there is reasonable agreement between the magnitudes of Strouhal numbers presented here ($1440 \leqslant Re \leqslant 1680$) and those reported by Sumner ($Re = 3.2 \times 10^4$–7.2×10^4) despite the difference in Reynolds number of over an order of magnitude. Conversely, at $Re = 5.5 \times 10^4$ with $P/D = 2.0$, Alam and Sakamoto (2005) and Alam et al. (2005) obtained Strouhal numbers of 0.47 and 0.09 for $\alpha = 8°$ and 12°, respectively. Furthermore, at $\alpha = 10°$ they obtained a bistable flow which switched between these two Strouhal numbers. The authors of the present paper do not have an explanation for the large discrepancy in Strouhal numbers obtained by Sumner et al. and Alam et al. for almost identical flow conditions.

3.2. Oscillating cylinders

In these experiments the upstream cylinder was oscillated transverse to the flow with peak-to-peak amplitude of $0.44D$ at various frequencies in the range $0.05 \leqslant f_e D/U \leqslant 0.44$. The flow velocity was kept approximately constant (ranging from 95 to 105 mm/s), and the variation in $f_e D/U$ was obtained by altering the oscillation frequency (the exact value of U was used to calculate $f_e D/U$). In addition to the flow visualization experiments, spectral measurements of the wake velocity were also obtained. It should be appreciated that for this range of $f_e D/U$ the maximum oscillatory velocity of the upstream cylinder is significant, varying from 7% to 61% of the freestream velocity as $f_e D/U$ varies from 0.05 to 0.44. On the basis of quasi-static considerations this gives a maximum induced incidence of the resultant velocity vector of between 4° and 31° with respect to the freestream velocity.

A summary of the wake flow spectra for the complete range of $f_e D/U$ is presented in 3-D form in Fig. 5; some sample 2-D plots for specific values of $f_e D/U$ are shown in Fig. 6 (the spectra are in arbitrary units, but the scale is constant for all measurements). In almost all cases the wake spectra contain a relatively small number of distinct peaks. The frequencies of these distinct peaks are designated as f_o; they are plotted in nondimensional form, $f_o D/U$, as a function of $f_e D/U$ in Fig. 7(a). The magnitude of the dominant of the distinct peaks is presented in Fig. 7(b) as a function of $f_e D/U$. In Fig. 7(a), lines showing integral relationships between wake and excitation frequency are drawn ($f_o = f_e/3$, $f_o = f_e/2$, $f_o = f_e$, $f_o = 2f_e$ and $f_o = 3f_e$); it is stressed that these lines do not represent curve fitting of the experimental data, they are drawn merely to help in the interpretation of the data.

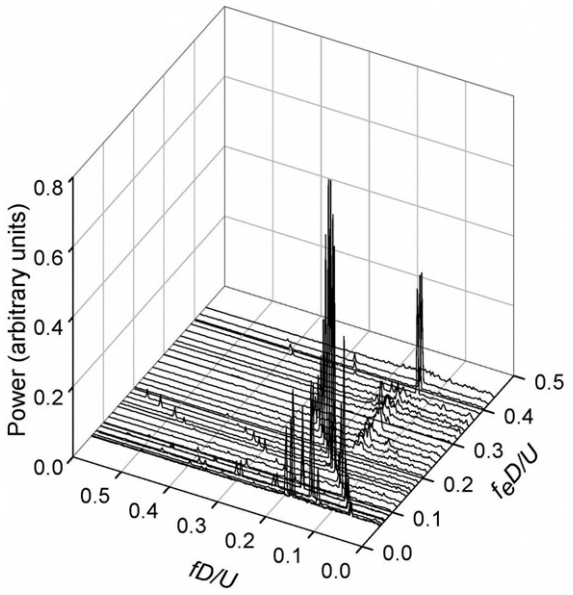

Fig. 5. Three-dimensional plot of wake power spectra as a function of excitation frequency, f_e.

As can be seen from Fig. 7, there are five different regions where the wake resonates with either the excitation frequency of the upstream cylinder or one of its sub- or superharmonics. These resonances are particularly apparent from the variation of the magnitude of the dominant wake peak with f_eD/U in Fig. 7(b). The flow phenomena associated with these five distinct regions are discussed individually in the following sections.

3.2.1. $\frac{1}{3}$-*Subharmonic synchronization*

For $0.053 \leqslant f_eD/U \leqslant 0.062$ the dominant peak in the power spectra is at three times the excitation frequency (see Figs. 5 and 7). Hence, three cycles of vortex street propagation occur for every cycle of cylinder oscillation, indicating that the wake has a $\frac{1}{3}$-subharmonic synchronization or period-three motion with respect to the upstream cylinder excitation. The dominance of the $3f_e$ peak is more obvious from the individual power spectra; an example of which is shown in Fig. 6(a) for $f_eD/U = 0.062$, with the dominant peak appearing at $f_oD/U = 0.18$. As indicated in Fig. 7(b), it appears that the resonance between wake structure and cylinder oscillation exists for frequencies below $f_eD/U = 0.053$, but it is not possible to do satisfactory experiments in this case (while maintaining a constant Re).

A series of video images, one every 1/8th of the period of the upstream cylinder oscillation, showing the flow evolution over one period of cylinder oscillation for $\frac{1}{3}$-subharmonic synchronization is given in Fig. 8 for $f_eD/U = 0.053$. (In this and all similar figures the position of maximum T/D is identified "by eye" from the video recording, and all other values of T/D are then calculated using the timing of the video frames. Also in all the video images presented in this paper the cylinders are "highlighted" to better show their location.) The period-three motion occurs only in the combined wake behind both cylinders. An examination of the wake behind the upstream cylinder (but upstream of the downstream cylinder) shows that there is only one cycle of wake motion per cycle of cylinder oscillation, as clearly identified by considering the two shear-layers shed from the upstream cylinder. In Figs. 8(a)–(c) (T/D decreasing from 0.39 to 0.17) the shear-layer shed from the lower surface of the upstream cylinder is deflected up across the face of the downstream cylinder. Fig. 8(d) shows this shear-layer reattaching onto the lower surface of the downstream cylinder; separation of this shear-layer from the downstream cylinder occurs in Fig. 8(e). As the upstream cylinder continues its motion, giving an increasing T/D, this shear-layer then reattaches at $T/D = 0.17$ (Fig. 8(g)), and is again deflected up across the face of the downstream cylinder in Fig. 8(i).

In contrast to the flow pattern discerned from the shear-layers shed from the upstream cylinder, examination of the vortices shed from the lower surface of the downstream cylinder shows that *three* vortices are shed during one period of the upstream cylinder motion. As shown in Fig. 8(a), a vortex has just formed for $T/D = 0.39$ (representing the maximum transverse separation between cylinders). The formation of the second vortex is shown at $T/D = 0.17$ in Fig. 8(c). The third and final vortex of the cycle is shown being formed at $T/D = 0.01$ in Fig. 8(f). It is evident that the

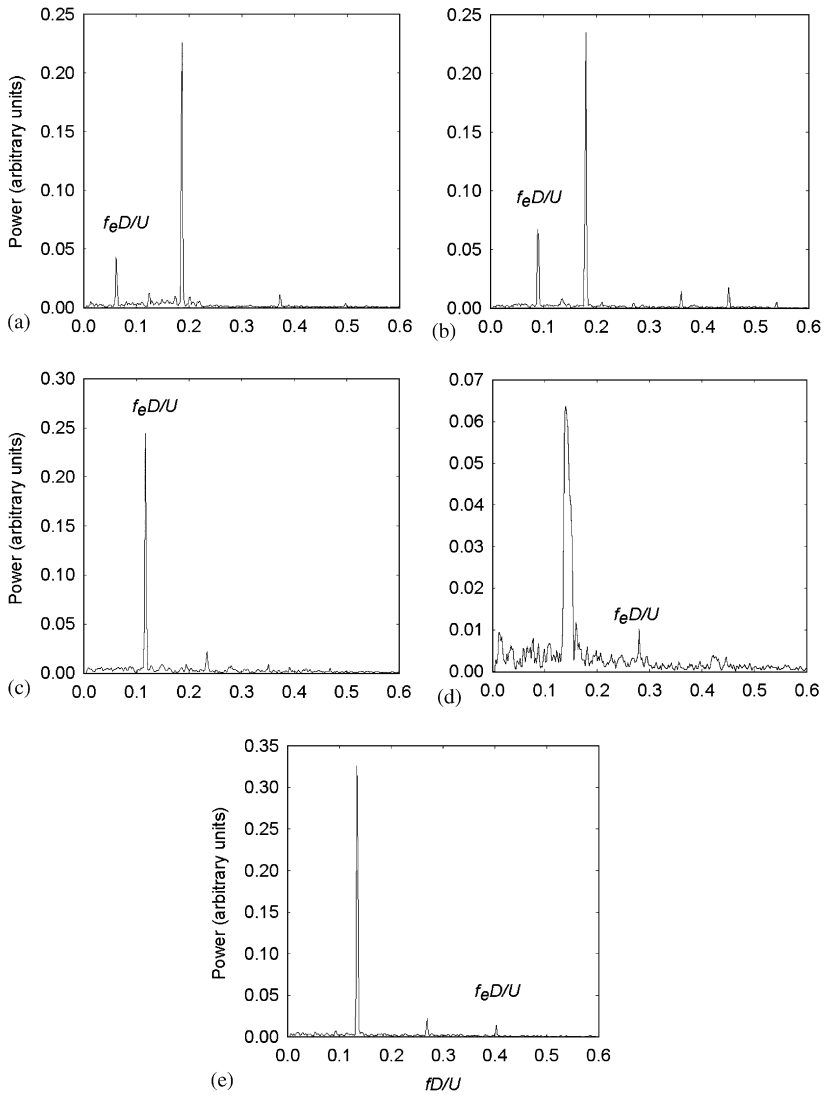

Fig. 6. Sample two-dimensional plots of the wake power spectra as a function of excitation frequency: (a) $f_eD/U = 0.062$; (b) $f_eD/U = 0.090$; (c) $f_eD/U = 0.117$; (d) $f_eD/U = 0.279$; (e) $f_eD/U = 0.402$.

formation of this vortex is associated with the separation of the shear-layer from the lower surface of the downstream cylinder; hence, it should be noted that the mechanism producing this vortex is very different to that for the other two vortices of the cycle.

The formation of the vortices from the upper surface of the downstream cylinder is not particularly clear from the images shown in Fig. 8, which are concentrated in the near-wake behind the cylinders. However, if we examine a wider view of the wake, as shown in Fig. 9 for one instant of the period, then it is apparent that a vortex is formed from the upper surface of the downstream cylinder which envelopes the vortices formed from the lower surface.

Another significant characteristic of the flow for this frequency of oscillation is that there is considerable hysteresis in the wake structure, depending on whether T/D is increasing or decreasing. For example, at $T/D = 0.17$ the flow belongs to the IS regime for decreasing T/D (Fig. 8(c)), but to the SLR regime for increasing T/D (Fig. 8(g)). Thinking quasi-statically a decreasing T/D implies a relative velocity vector directed away from the downstream cylinder, hence there is an increase in the apparent value of T/D; while an increasing T/D has the reverse effect, giving a decrease in the apparent value of T/D. This is consistent with a decreasing T/D producing an IS type flow (associated with higher values of T/D for stationary cylinders) and an increasing T/D producing a SLR type flow (associated with lower values of T/D for stationary cylinders). It should also be pointed out that the period-three motion in the wake behind the two

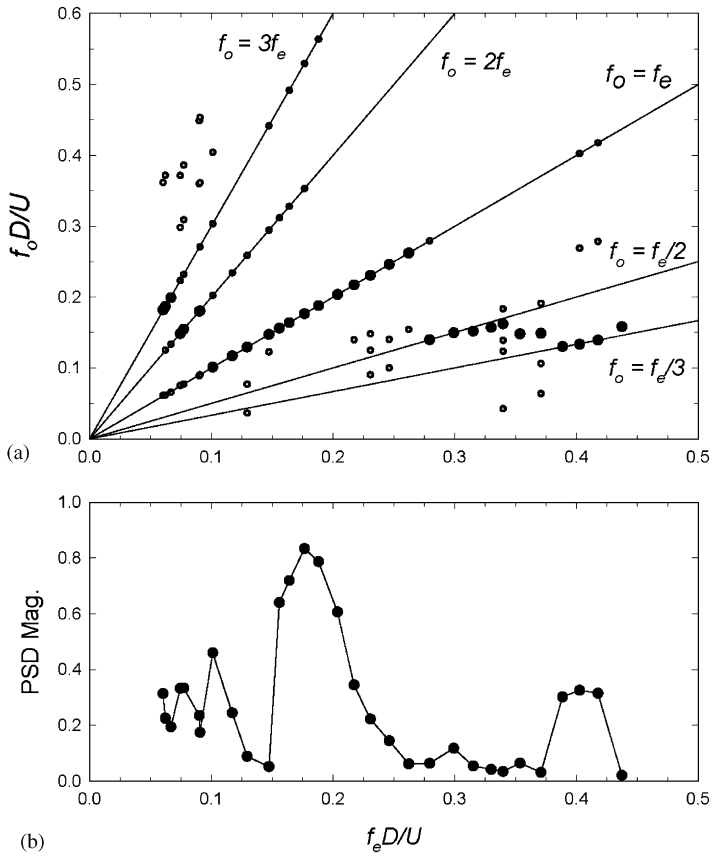

Fig. 7. Identification of distinct peaks extracted from the wake spectra shown in Fig. 5: (a) •, frequency of dominant peak; ◦, other distinct peaks in spectra; —— lines showing integral relationships between wake frequency and excitation frequency; (b) magnitude of dominant peak in (a).

cylinders does not represent three identical flow patterns repeating one after another; instead, during one cycle of cylinder motion three vortices are formed by quite different mechanisms from the lower surface of the downstream cylinder.

3.2.2. $\frac{1}{2}$-*Subharmonic synchronization*

For $0.074 \leqslant f_eD/U \leqslant 0.090$, the near-wake switched to a $\frac{1}{2}$-subharmonic synchronization (see Figs. 5 and 7), with the dominant periodicity in the wake occurring at twice the excitation frequency; a typical plot of the wake spectra for this case is shown in Fig. 6(b) for $f_eD/U = 0.090$, with the dominant peak at $f_oD/U = 0.18$. Interestingly, the results of Williamson and Roshko (1988) indicate that a stable vortex street cannot occur for $\frac{1}{2}$-subharmonic excitation. Possibly, the presence of the downstream cylinder enables a stable wake pattern with $\frac{1}{2}$-subharmonic excitation to be obtained.

A set of flow visualization images over one complete cycle of cylinder excitation for the $\frac{1}{2}$-subharmonic synchronization is shown in Fig. 10 for $f_eD/U = 0.080$. In common with the flow visualization obtained for the $\frac{1}{3}$-subharmonic synchronization at $f_eD/U = 0.053$ (Fig. 8), although the flow downstream of the two cylinders is period-two, the flow between the cylinders is clearly period one, as can be ascertained by examining the shear-layers shed from the upstream cylinder.

The period-two motion of the wake behind the cylinders can be seen from the vortices shed from the lower surface of the downstream one. The first vortex is just starting to form at $T/D = 0.39$, as shown in Fig. 10(a); it is then shed in the interval between Figs. 10(c) and (d). The second vortex is formed between $T/D = 0.01$ and 0.17, see Figs. 10(f) and (g); it is associated with the shear-layer separation from the lower surface of the downstream cylinder, which also occurs in this time interval, although slightly in advance of the vortex formation process.

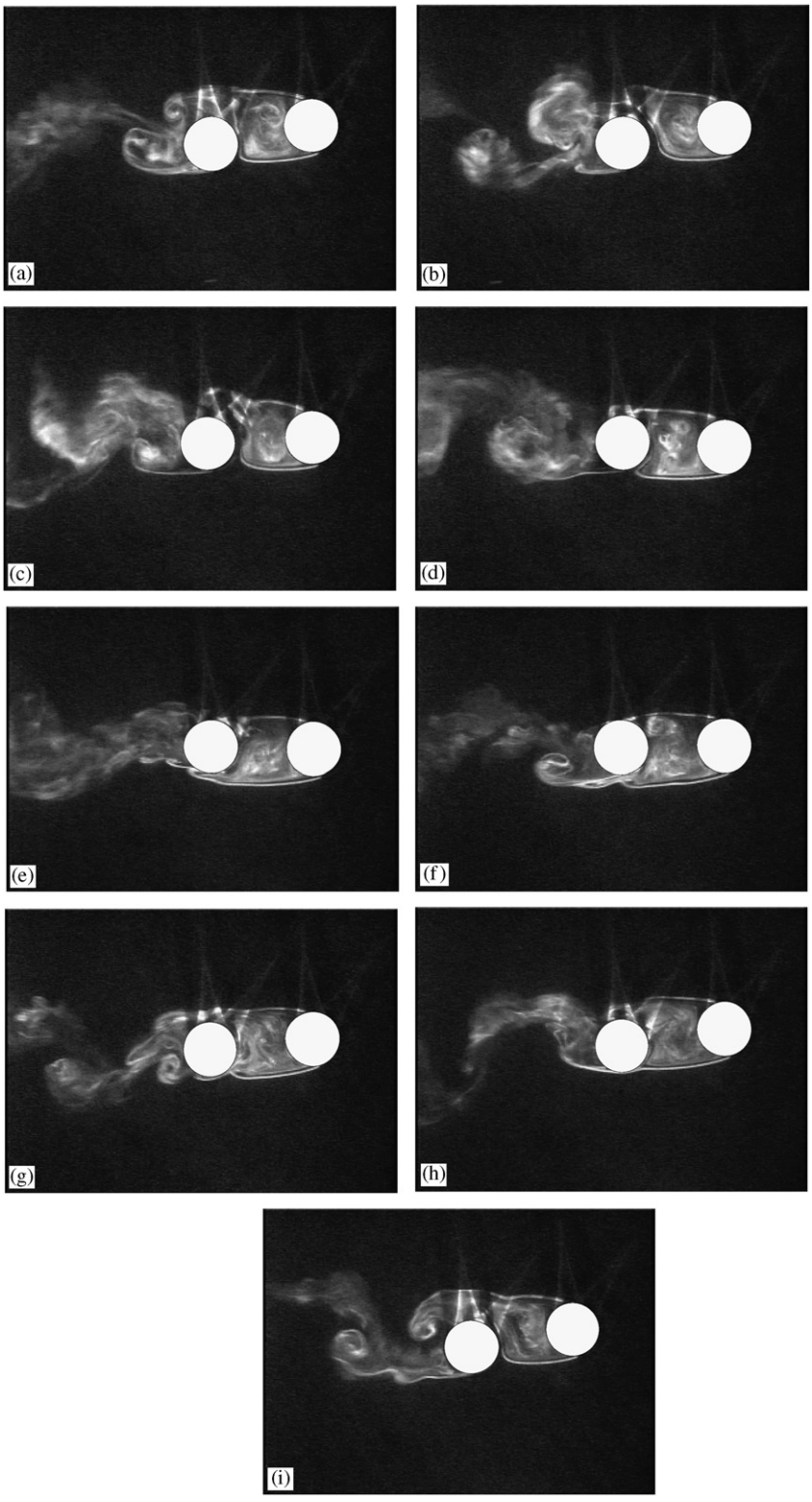

Fig. 8. Flow visualization images showing $\frac{1}{3}$-subharmonic synchronization with the upstream cylinder oscillating at $f_e D/U = 0.053$; one complete cycle of oscillation of the upstream cylinder is shown. The instantaneous values of transverse separation between cylinders, T/D, and time as a fraction of the period of oscillation of the upstream cylinder, t/P^*, are as follows: (a) $T/D = 0.39$, $t/P^* = 0.0$; (b) $T/D = 0.33$, $t/P^* = 0.13$; (c) $T/D = 0.17$, $t/P^* = 0.25$; (d) $T/D = 0.01$, $t/P^* = 0.38$; (e) $T/D = -0.05$, $t/P^* = 0.5$; (f) $T/D = 0.01$, $t/P^* = 0.63$; (g) $T/D = 0.17$, $t/P^* = 0.75$; (h) $T/D = 0.33$, $t/P^* = 0.88$; (i) $T/D = 0.39$, $t/P^* = 1.0$.

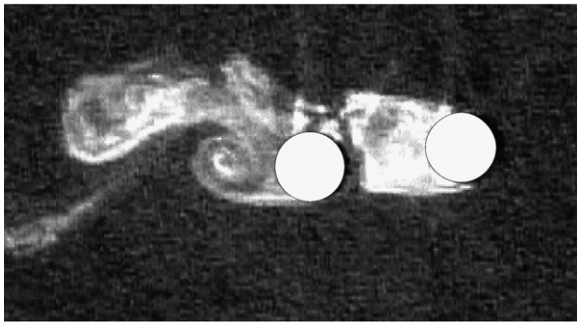

Fig. 9. Global wake flow visualization image with the upstream cylinder oscillating at $f_eD/U = 0.053$.

Also in common with the $\frac{1}{3}$-subharmonic synchronization, in this case also we see combinations of both the IS and SLR flow regimes. When $T/D \geqslant 0.33$, the visualization shows flow patterns consistent with the IS regime, while for $T/D \leqslant 0.0$ (Figs. 10(e) and (f)) the flow is easily identified as SLR. Further, in common with $\frac{1}{3}$-subharmonic synchronization, there is considerable hysteresis in the flow. For example, at $T/D = 0.17$ the flow for increasing T/D (Fig. 10(g)) is representative of the SLR regime, while for decreasing T/D (Fig. 10(c)) it is much more representative of the IS regime; this is consistent with the results obtained for the $\frac{1}{3}$-subharmonic synchronization, and can be explained using the same quasi-static arguments as in Section 3.2.1.

3.2.3. *Fundamental lock-in*

A fundamental lock-in with the dominant wake frequency equal to the excitation frequency exists for $0.101 \leqslant f_eD/U \leqslant 0.246$, see Figs. 5 and 7; a typical plot of the power spectra for a fundamental lock-in at $f_eD/U = 0.117$ is shown in Fig. 6(c). In this range of excitation frequencies the shear-layers shed from the upstream cylinder roll-up to form vortices in the region between the cylinders. This is in complete contrast to what is observed for lower values of f_eD/U, where, although there are oscillations of the shear-layers shed from the upstream cylinder and recirculation of the flow in the gap between the cylinders, no vortices are formed in this gap. The vortices formed in the gap are then swept around the downstream cylinder; hence, the flow no longer bears any resemblance to either the IS or SLR type flow observed when the cylinders are stationary or oscillating with $f_eD/U < 0.1$.

As is apparent from Fig. 7(b), the region of f_eD/U corresponding to fundamental lock-in can be subdivided into two sub-regions, with a distinct minimum in the strength of the wake periodicity at $f_eD/U \approx 0.15$. For the lower frequency range, $0.101 \leqslant f_eD/U \leqslant 0.147$, the timing of the vortices swept around the downstream cylinder relative to those shed from the downstream cylinder itself is such that two pairs of vortices are formed on either side of the combined wake. Hence, the wake is very similar to the 2P wake proposed by Williamson and Roshko (1988), although, of course, the mechanism producing the 2P wake here is very different to that observed by Williamson and Roshko for a single oscillating cylinder. A set of video images for this type of flow is shown in Fig. 11 for $f_eD/U = 0.144$; note, as indicated in the figure caption, this set of images is not for equal intervals of time; also much more of the wake is shown here than in previous images. As shown in Fig. 11(a), where T/D is a maximum, a vortex has just separated from the upper surface of the upstream cylinder and a second vortex is starting to form on the upper surface of the downstream cylinder. The former is swept around the latter, as shown in Fig. 11(b); this and the vortex shed from the upper surface of the downstream cylinder then combine to form a pair of vortices in the combined wake of the two cylinders at $T/D = -0.05$, see Fig. 11(c). (The same process can be seen occurring on the lower surface of the downstream cylinder; however, the process is not as pronounced, reflecting the difference in area of the downstream cylinder which is exposed to the flow for the maximum and minimum T/D.)

For the higher range of frequencies within the fundamental lock-in range, $0.147 < f_eD/U \leqslant 0.246$, it is not possible to distinguish the vortices shed from the downstream cylinder itself from those originating from the upstream cylinder, and the wake is now more characteristic of a 2S wake. It appears that the vortices shed from the upstream cylinder strengthen the vortex-shedding process from the downstream one; hence, the much stronger resonance in the wake for this range of f_eD/U. A set of video images for this type of flow presented in Fig. 12 for $f_eD/U = 0.159$ shows only one vortex on each side of the wake downstream of the pair of cylinders.

In both of these ranges of excitation frequency there is still considerable hysteresis in the flow and, as can be seen from Figs. 11 and 12, very different flow patterns are obtained for the same T/D, depending on whether T/D is

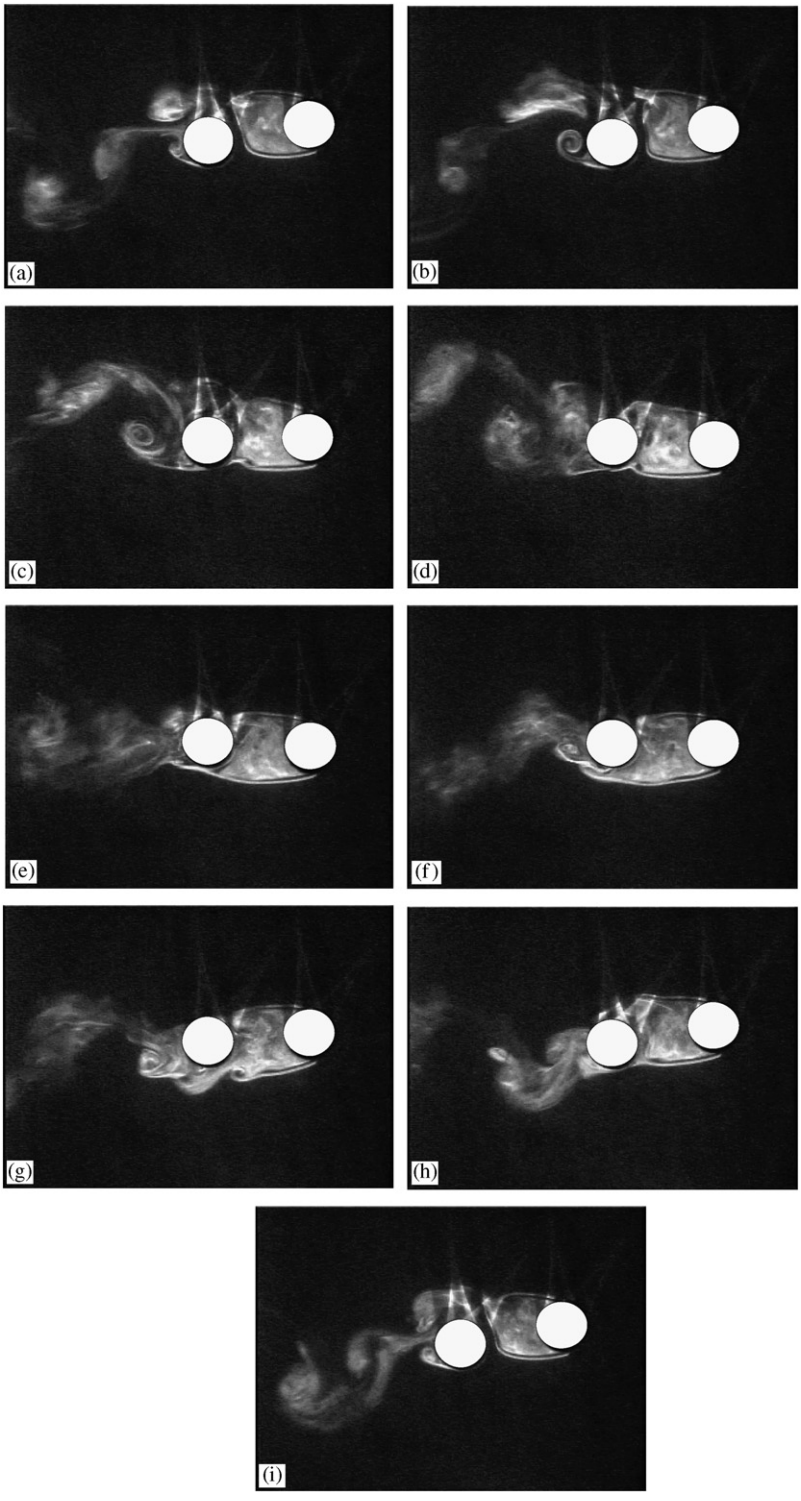

Fig. 10. Flow visualization images showing $\frac{1}{2}$-subharmonic synchronization with the upstream cylinder oscillating at $f_e D/U = 0.080$; one complete cycle of oscillation of the upstream is shown. The instantaneous values of transverse separation between cylinders, T/D, and time as a fraction of the period of oscillation of the upstream cylinder, t/P^*, are as follows: (a) $T/D = 0.39$, $t/P^* = 0.0$; (b) $T/D = 0.33$, $t/P^* = 0.13$; (c) $T/D = 0.17$, $t/P^* = 0.25$; (d) $T/D = 0.01$, $t/P^* = 0.38$; (e) $T/D = -0.05$, $t/P^* = 0.5$; (f) $T/D = 0.01$, $t/P^* = 0.63$; (g) $T/D = 0.17$, $t/P^* = 0.75$; (h) $T/D = 0.33$, $t/P^* = 0.88$; (i) $T/D = 0.39$, $t/P^* = 1.0$.

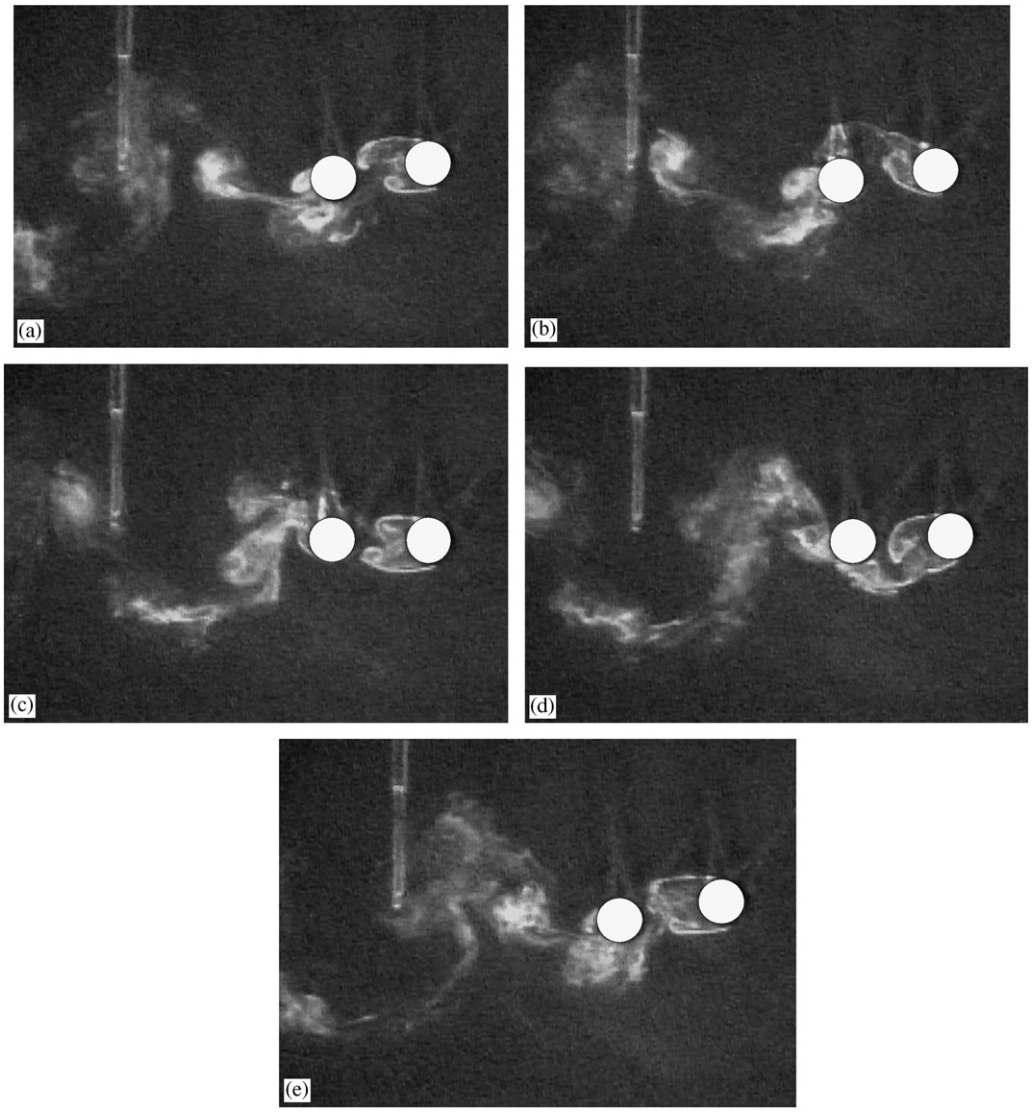

Fig. 11. Flow visualization images during fundamental lock-in with the upstream cylinder oscillating at $f_eD/U = 0.144$; one complete cycle of oscillation of the upstream cylinder is shown. The instantaneous values of transverse separation between cylinders, T/D, and time as a fraction of the period of oscillation of the upstream cylinder, t/P^*, are as follows: (a) $T/D = 0.39$, $t/P^* = 0.0$; (b) $T/D = 0.21$, $t/P^* = 0.21$; (c) $T/D = -0.05$, $t/P^* = 0.52$; (d) $T/D = 0.18$, $t/P^* = 0.76$; (e) $T/D = 0.39$, $t/P^* = 1.0$.

increasing or decreasing. Once again the difference in flow patterns for increasing and decreasing T/D can be explained using a quasi-static arguments. In both Figs. 11(b) and 12(b), where T/D is decreasing, the resultant velocity vector (accounting for both the freestream velocity and component normal to the oscillating cylinder) is directed upwards and the near-wake behind the upstream cylinder is seen to be shed in this direction. Conversely, for both Figs. 11(d) and 12(d), where T/D is increasing, the resultant velocity vector is directed downwards, and again the wake favours this direction.

3.2.4. 2-superharmonic synchronization

When f_e is increased beyond the fundamental lock-in range, the wake spectra indicate a very weak two-superharmonic synchronization, with $f_o = f_e/2$, for $0.279 \leqslant f_eD/U \leqslant 0.299$ (Figs. 5 and 7(b)). A typical plot of the power

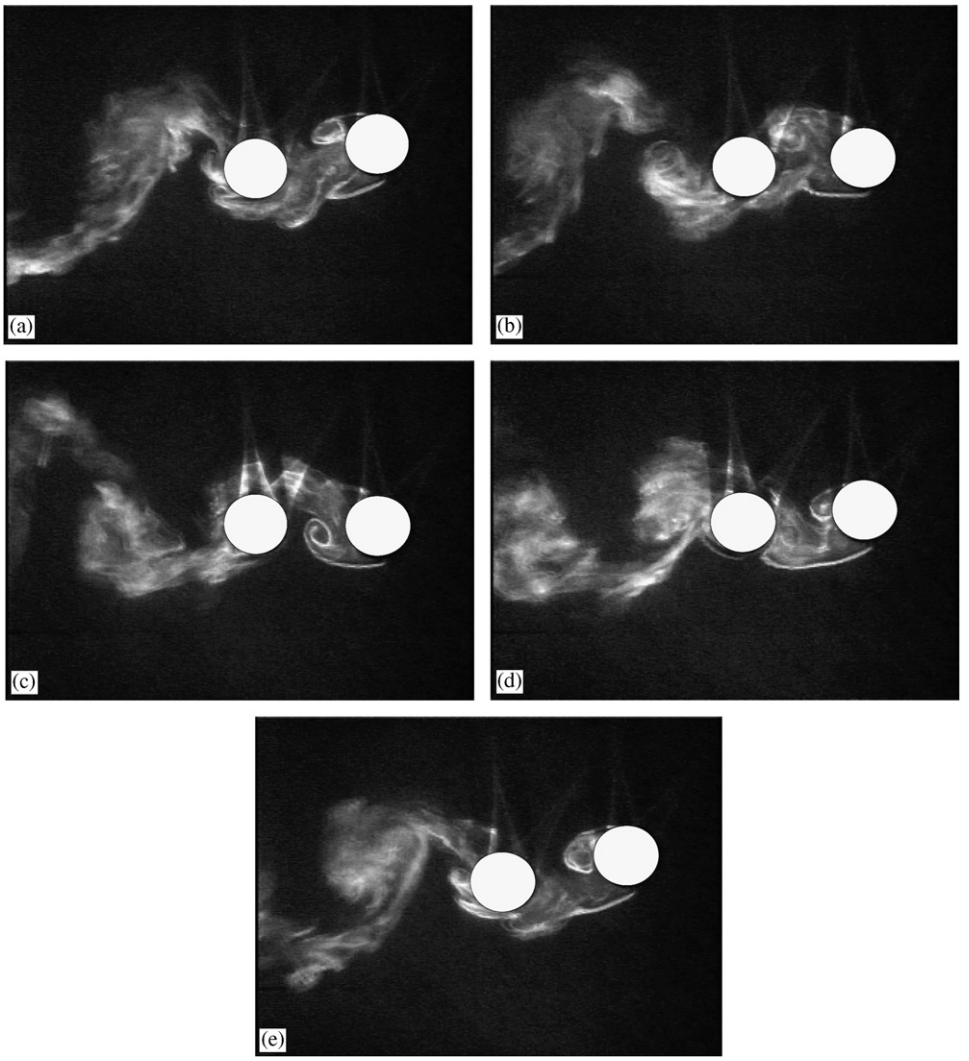

Fig. 12. Flow visualization images during fundamental lock-in showing a 2S wake pattern with the upstream cylinder oscillating at $f_eD/U = 0.159$; one complete cycle of oscillation of the upstream cylinder is shown. The instantaneous values of transverse separation between cylinders, T/D, and time as a fraction of the period of oscillation of the upstream cylinder, t/P^*, are as follows: (a) $T/D = 0.39$, $t/P^* = 0.0$; (b) $T/D = 0.17$, $t/P^* = 0.25$; (c) $T/D = -0.05$, $t/P^* = 0.5$; (d) $T/D = 0.17$, $t/P^* = 0.75$; (e) $T/D = 0.39$, $t/P^* = 1.0$.

spectra for a 2-superharmonic synchronization at $f_eD/U = 0.279$ is shown in Fig. 6(d). From the flow visualization it is not possible to identify any clear relationship between the vortices shed from the downstream cylinder and the oscillation of the upstream cylinder, and hence no images are presented. There was, however, a clearly defined vortex street downstream of the pair of cylinders.

3.2.5. 3-superharmonic synchronization

Finally, a much stronger 3-superharmonic synchronization, $f_o = f_e/3$, occurred for $0.388 \leqslant f_eD/U \leqslant 0.417$ (Figs. 5 and 7(b)). A typical plot of the power spectra at $f_eD/U = 0.402$ is shown in Fig. 6(e). A series of typical flow-visualization images is shown in Fig. 13 for $f_eD/U = 0.389$. These images cover three cycles of oscillation for the upstream cylinder and, hence, show one period of the vortex formation process in the wake of the two cylinders; Figs. 13(a)–(e) show one period of oscillation for the upstream cylinder.

The formation of the wake vortices can clearly be seen from the visualization images. Fig. 13(a), $T/D = 0.39$, shows a vortex in the process of being formed on the lower surface of the downstream cylinder. This vortex is shed in the

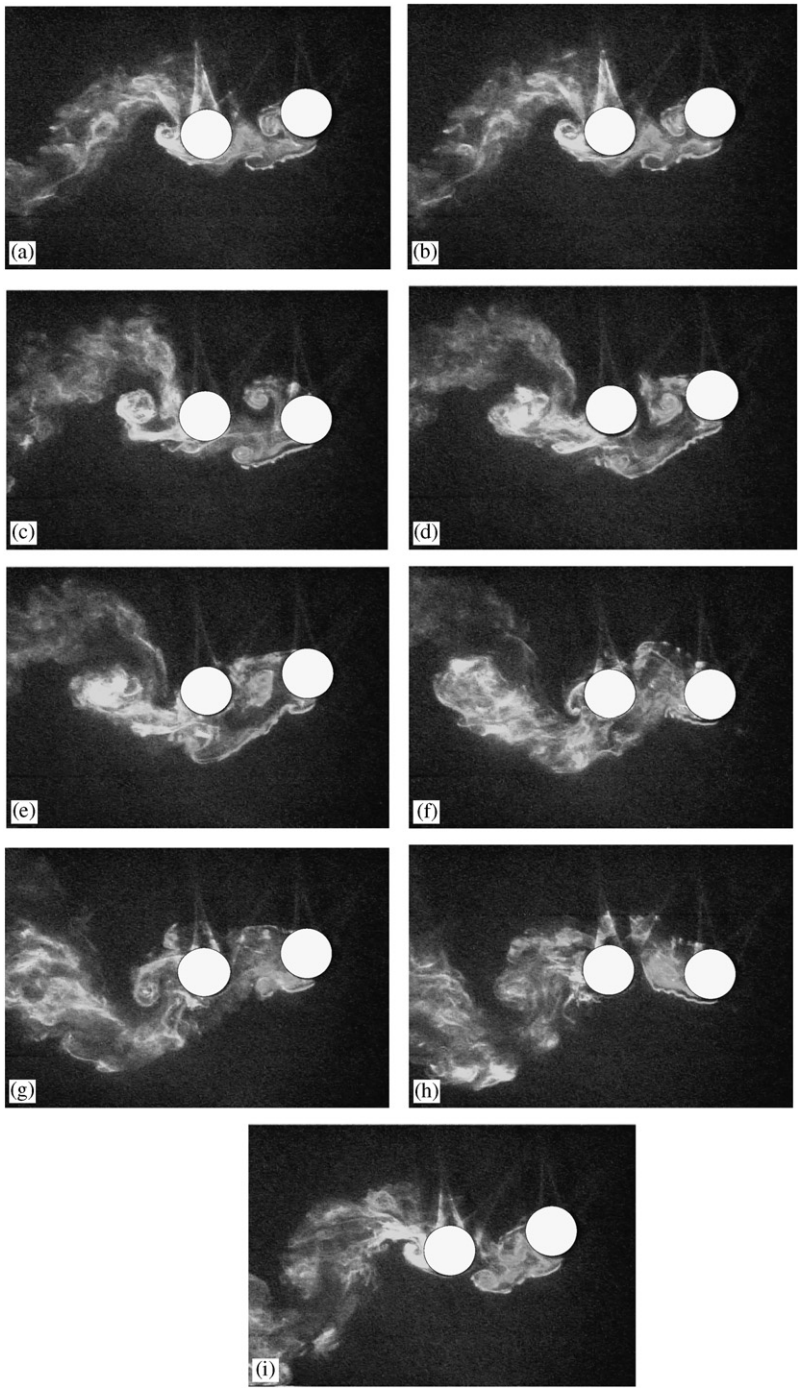

Fig. 13. Flow visualization images showing 3-superharmonic synchronization with the upstream cylinder oscillating at $f_e D/U = 0.389$; three complete cycles of oscillation of the upstream cylinder are shown. The instantaneous values of transverse separation between cylinders, T/D, and time as a fraction of the period of oscillation of the upstream cylinder, t/P^*, are as follows: (a) $T/D = 0.39$, $t/P^* = 0.0$; (b) $T/D = 0.36$, $t/P^* = 0.08$; (c) $T/D = 017$, $t/P^* = 0.51$; (d) $T/D = 0.27$, $t/P^* = 0.83$; (e) $T/D = 0.39$, $t/P^* = 0.99$; (f) $T/D = -0.05$, $t/P^* = 1.49$; (g) $T/D = 0.39$, $t/P^* = 1.97$; (h) $T/D = -0.05$, $t/P^* = 2.48$; (i) $T/D = 0.39$, $t/P^* = 2.99$.

interval between $T/D = 0.36$ and 0.17, see Figs. 13(b) and (c). The vortex from the upper surface of the downstream cylinder can be seen starting to form in Fig. 13(f), and its separation and movement downstream is shown in Figs. 13(g) and (h).

Although only one pair of vortices are shed downstream of the cylinder pair for every three cycles of the upstream cylinder, it appears that three sets of vortex pairs are shed in the gap between the cylinders during this time—one for each period of the upstream cylinder. This can be seen most clearly by observing the vortices shed from the lower surface of the upstream cylinder. Fig. 13(a) shows the first vortex just shed at $T/D = 0.39$; for $T/D = 0.36$, as shown in Fig. 13(b), this vortex is being swept around the lower surface of the downstream cylinder, and a new vortex is being formed on the lower surface of the upstream cylinder. Fig. 13(d) shows this second vortex being swept around the lower surface of the downstream cylinder, and finally, Figs. 13(e) and (f) ($T/D = 0.39$ and -0.05), show the formation of the third vortex on the lower surface of the upstream cylinder.

4. Conclusions

The flow around a pair of staggered cylinders, with $L/D = 2.0$ and $T_{\mathrm{nom}}/D = 0.17$, subjected to forced transverse oscillation of the upstream cylinder, giving $-0.05 \leqslant T/D \leqslant 0.39$, has been studied experimentally for the Reynolds number range $1440 \leqslant \mathrm{Re} \leqslant 1680$. This configuration is completely within the range of "small incidence" type flows of Sumner et al. (2000). The flow regime is shown to be strongly dependent on the value of T/D.

When the cylinders are stationary, for most of the range of T/D the flow regime is of the SLR type, where the shear-layers shed from the upstream cylinder attach to the surface of the downstream cylinder in a manner synchronized with the vortex-shedding process. However, when T/D is close to its maximum value, the resulting flow regime is of the IS type, where the inner shear-layer shed from the upstream cylinder is deflected through the gap between the cylinders.

The flow downstream of the pair of cylinders was investigated with the upstream cylinder forced to oscillate sinusoidally, transverse to the flow direction, in the frequency range $0.053 \leqslant f_e D/U \leqslant 0.44$. Within this excitation range the wake exhibited strong periodicities at the frequency of the oscillating cylinder, and five distinct regions of synchronization were obtained between these wake periodicities and the frequency of oscillation of the upstream cylinder; these regions included both sub- and superharmonic resonances, as well as the usual fundamental lock-in.

$\frac{1}{3}$- and $\frac{1}{2}$-subharmonic synchronization regions were obtained for $0.053 \leqslant f_e D/U \leqslant 0.062$ and $0.074 \leqslant f_e D/U \leqslant 0.090$, respectively. In these regions no vortices are formed in the gap between the two cylinders, although there are oscillations of the shear-layers shed from the upstream cylinder, occurring at the frequency of oscillation of the upstream cylinder as opposed to the frequency of vortex shedding in the wake of the two cylinders. On the other hand, a clear vortex street is formed downstream of the lee cylinder. Furthermore, regions of SLR and IS flows are evident for both of these synchronization regions; however, there is considerable hysteresis in the flow, with different flow regimes occurring for the same value of T/D, depending on whether T/D is increasing or decreasing. Another common feature of the $\frac{1}{3}$- and $\frac{1}{2}$-subharmonic synchronization regions is that, although three and two vortices are produced, respectively, in the wake behind the cylinder pair per cycle of cylinder oscillation, this does not represent three or two identical flow patterns repeating one after another. Instead, the vortices are formed by quite different mechanisms during the period of the upstream cylinder oscillation.

The range of excitation frequencies for fundamental synchronization was much larger for a pair of cylinders, $0.101 \leqslant f_e D/U \leqslant 0.246$, compared to that obtained in the same experimental facility for a single cylinder, $0.16 \leqslant f_e D/U \leqslant 0.20$ (Krishnamoorthy et al., 2001). This effect has also been observed by Mahir and Rockwell (1996a, b) in their experimental study where both cylinders are oscillating. Within the lock-in range, the shear-layers shed from the upstream cylinder form vortices in the region between the cylinders which are then swept around the downstream cylinder; hence, this flow no longer has any resemblance to either the SLR or IS type flows.

It was found that the fundamental lock-in region can be subdivided into two sub-regions, the difference between them being the timing of the vortices shed from the two cylinders. In the lower-frequency sub-region range the timing is such that two pairs of vortices are shed per cycle of oscillation, and hence the wake resembles the 2P wake of Williamson and Roshko (1988). In the higher-frequency sub-range the timing of the vortices shed from the upstream cylinder is such that they coalesce with those from the downstream cylinder, and hence only two single vortices are shed per cycle of oscillation. This vortex coalescence is reflected in a much stronger resonance in the wake for this sub-region of the fundamental lock-in.

For frequencies greater than the fundamental lock-in range, 2- and 3-superharmonic synchronization flows were obtained for $0.279 \leqslant f_e D/U \leqslant 0.299$ and $0.388 \leqslant f_e D/U \leqslant 0.417$, respectively. The former was relatively weak; however, a much stronger 3-superharmonic synchronization was obtained. In common with the fundamental lock-in, both the

2- and 3-superharmonic synchronization regions exhibited the formation of vortices in the gap between the cylinders and, hence, the flow no longer shared any characteristics with either the IS or SLR flows.

It should be stressed that although only $\frac{1}{3}$-subharmonic to 3-superharmonic synchronization regions were obtained in this set of experiments, this does not imply that lower subharmonic or higher superharmonic synchronizations do not exist. It is quite possible that other synchronization regions may be found if the range of frequency excitation is extended beyond that for which the present experimental apparatus is capable.

Although detailed measurements of the vortex formation length were not conducted in these experiments, it appears that this was a minimum for the 3-superharmonic synchronization. This was also the case for a solitary oscillating cylinder (Krishnamoorthy et al., 2001).

The results presented in this paper are for the Reynolds number range $1440 \leqslant Re \leqslant 1680$. It is well known that for a single stationary cylinder the wake is strongly dependent on Reynolds number. For example, the flow visualization results of Unal and Rockwell (1988) show that the length of the wake formation region increases with increasing Re for $Re < 2000$, and then progressively decreases as Re in increased above 2000. The results presented here indicate that there is reasonable agreement in the Strouhal numbers measured with those measured at Re over an order of magnitude greater (Sumner and Richards, 2003; Sumner et al., 2005; Sumner, 2006). Despite this, in common with the flow around a stationary cylinder, it is to be expected that the size of the wake region for a pair of cylinders will be strongly influenced by Reynolds number, and hence the existence and range of the various synchronization regimes described in this paper may well be dependent on the specific value of Re.

Acknowledegments

The authors gratefully acknowledge the support by the Natural Sciences and Engineering Research Council (NSERC) of Canada.

References

Alam, M.M., Sakamoto, H., 2005. Investigation of Strouhal frequencies of two staggered bluff bodies and detection of multistable flow by wavelets. Journal of Fluids and Structures 20, 425–449.

Alam, M.M., Sakamoto, H., Zhou, Y., 2005. Determination of flow configurations and fluid forces acting on two staggered circular cylinders of equal diameter in cross-flow. Journal of Fluids and Structures 21, 363–394.

Bearman, P.W., Currie, I.G., 1979. Pressure-fluctuation measurements on an oscillating circular cylinder. Journal of Fluid Mechanics 91, 661–677.

Blackburn, H.M., Henderson, R.D., 1999. A study of two-dimensional flow past an oscillating cylinder. Journal of Fluid Mechanics 385, 255–286.

Bouak, F., Lemay, J., 1998. Passive control of the aerodynamic forces acting on a circular cylinder. Experimental Thermal and Fluid Science 16, 112–121.

Brika, D., Laneville, A., 1993. Vortex-induced vibrations of a long flexible cylinder. Journal of Fluid Mechanics 250, 481–508.

Carberry, J., Sheridan, J., Rockwell, D., 2001. Forces and wake modes of an oscillating cylinder. Journal of Fluids and Structures 15, 523–532.

Feng, C.C., 1968. The measurement of vortex-induced effects in flow past stationary and oscillating circular and D-section cylinders. Master's Thesis, University of British Columbia, Canada.

Gu, W., Chyu, C., Rockwell, D., 1994. Timing of vortex formation from an oscillating cylinder. Physics of Fluids 6, 3677–3682.

Gu, Z.F., Sun, T.F., 1999. On interference between two circular cylinders in staggered arrangement at high subcritical Reynolds numbers. Journal of Wind Engineering and Industrial Aerodynamics 80, 321–374.

Khalak, A., Williamson, C.H.K., 1997. Fluid forces and dynamics of a hydroelastic structure with very low mass and damping. Journal of Fluids and Structures 11, 973–982.

Krishnamoorthy, S., Price, S.J., Païdoussis, M.P., 2001. Cross-flow past an oscillating circular cylinder: synchronization phenomena in the near wake. Journal of Fluids and Structures 15, 955–980.

Koopmann, G.H., 1967. The vortex wakes of vibrating cylinders at low Reynolds numbers. Journal of Fluid Mechanics 28, 501–512.

Lai, W.C., Zhou, Y., So, R.M.C., Wang, T., 2003. Interference between stationary and vibrating cylinder wakes. Physics of Fluids 15, 1687–1695.

Lu, X.-Y., Dalton, C., 1996. Calculation of the timing of vortex formation from an oscillating cylinder. Journal of Fluids and Structures 10, 527–541.

Mahir, M., Rockwell, D., 1996a. Vortex formation from a forced system of two cylinders. Part I: tandem arrangement. Journal of Fluids and Structures 10, 473–489.

Mahir, M., Rockwell, D., 1996b. Vortex formation from a forced system of two cylinders. Part II: side-by-side arrangement. Journal of Fluids and Structures 10, 491–500.
Nishimura, T., 1986. Flow across tube banks. In: Cheremisinoff, N.P. (Ed.), Encyclopedia of Fluid Mechanics—Flow Phenomena and Measurement, vol. 1. Gulf, pp. 763–785.
Ohya, Y.O., Okajima, A., Hayashi, M., 1989. Wake interference and vortex shedding. In: Cheremisinoff, N.P. (Ed.), Encyclopedia of Fluid Mechanics—Aerodynamics and Compressible Flow, vol. 8. Gulf, pp. 322–389.
Ongoren, A., Rockwell, D., 1988. Flow structure from an oscillating cylinder. Part 1. Mechanisms of Phase shift and recovery in the near wake. Journal of Fluid Mechanics 191, 197–223.
Stansby, P.K., 1976. The locking-of vortex shedding due to the cross-stream vibration of circular cylinders in uniform and shear flows. Journal of Fluid Mechanics 74, 641–655.
Sumner, D., Price, S.J., Païdoussis, M.P., 2000. Flow-pattern identification for two staggered circular cylinders in cross-flow. Journal of Fluid Mechanics 411, 263–303.
Sumner, D., Richards, M.D., 2003. Some vortex-shedding characteristics of the staggered configuration of circular cylinders. Journal of Fluids and Structures 17, 345–350.
Sumner, D., Richards, M.D., Akosile, O.O., 2005. Two staggered circular cylinders of equal diameter in cross-flow. Journal of Fluids and Structures 20, 255–276.
Sumner, D., 2006. Private communication.
Ting, D.S.K., Wang, D.J., Price, S.J., Païdoussis, M.P., 1998. An experimental study on the fluidelastic forces for two staggered circular cylinders in cross-flow. Journal of Fluids and Structures 12, 259–294.
Unal, M.F., Rockwell, D., 1988. On vortex formation from a cylinder. Part 1. The initial instability. Journal of Fluid Mechanics 190, 491–512.
Williamson, C.H.K., Roshko, A., 1988. Vortex formation in the wake of an oscillating cylinder. Journal of Fluids and Structures 2, 355–381.
Zdravkovich, M.M., 1987. The effects of interference between circular cylinders in cross flow. Journal of Fluids and Structures 1, 239–261.
Zdravkovich, M.M., 1993. Interstitial flow field and fluid forces. In: Au-Yang, M.K. (Ed.), Technology for the 90s: A Decade of Progress. ASME, New York.
Zhou, C.Y., So, R.M.C., Lam, K., 1999. Vortex-induced vibrations of an elastic circular cylinder. Journal of Fluids and Structures 13, 165–189.